Polarization studies of rare-gas resonance radiation: Argon, krypton, and xenon

C. Norén,* W. L. Karras,† and J. W. McConkey
Department of Physics, University of Windsor, Windsor, Ontario, Canada N9B 3P4

P. Hammond
Department of Physics, University of Manchester, Manchester M13 9PL, United Kingdom

(Received 19 December 1995)

The linear polarization of resonance vacuum-ultraviolet (VUV) radiation emitted by electron-impact excited Ar, Kr, and Xe atoms has been measured in the energy range from threshold to 480 eV using two sets of apparatus. The first apparatus measured the polarization function in the near-threshold region using an energy selected electron beam with a resolution of 160 meV. This enabled the effects of negative-ion resonances on the polarization function to be examined in detail. Predictions of the effects of negative-ion resonances on the observed polarizations have been made using a generalized Baranger-Gerjuoy theory. Excitation via electron exchange is shown to be a significant process very close to threshold. The second apparatus used an electron beam with ~1 eV resolution to probe the broad features of the VUV polarization functions over the energy range from threshold to 480 eV. Measurements are compared with other published data. [S1050-2947(96)04207-2]

PACS number(s): 34.80.Dp, 34.80.Nz, 42.25.Ja

I. INTRODUCTION

This paper is the third in a series of articles dealing with the polarization of the resonance radiation from the rare gases, particularly in the near-threshold region. The first two papers dealt with helium [1] and neon [2] and will be referred to as I and II, respectively. These give the background and motivation for this work and provide most of the necessary experimental and theoretical details. In this work data are presented using both energy-selected and -unselected electron beams. In the latter case the broad features of the vacuum-ultraviolet (VUV) polarization functions are measured over the energy range from threshold to 500 eV. Measurements made with the energy-selected beam (higher resolution) were confined to the first 5 eV above threshold where the influence of negative-ion resonances is most clearly observed. Other VUV polarization measurements have been performed by Dassen *et al.* [3] (104.8- and 106.7-nm lines of Ar), Al-Shamma and Kleinpoppen [4,5] (Kr and Xe), and Uhrig *et al.* [6,7] (Ne, Ar, Kr, and Xe). Some recent polarization measurements on visible and near-infrared transitions in the heavy rare gases have been reported by Furst *et al.* [8].

II. THEORY

Argon, krypton, and xenon have a similar coupling scheme and ion core parity that suggest that common features may be observed. As with neon (II), the jLS coupling scheme may be used to describe the first excited states. The orbital angular momentum (**L**) of the excited electron is coupled to the total angular momentum (**j**) of the ion core to form an intermediate state **K**, which in turn is coupled to the excited electron's spin (**S**) to form the total angular momentum (**J**) of the atom. The notation for describing these states is $(^{2s+1}l_j)^{2S+1}L[K]_J$, where **l** and **s** are orbital and spin angular momentum of the ion core, respectively. However, the lowest VUV-emitting states ($J=1$) can be considered as an admixture of ^1P and ^3P LS-coupled states and are represented as follows:

$$|(^2P_{1/2})^1S[\tfrac{1}{2}]_1\rangle = \alpha|^1P_1\rangle + \beta|^3P_1\rangle,$$

$$|(^2P_{3/2})^1S[\tfrac{3}{2}]_1\rangle = -\beta|^1P_1\rangle + \alpha|^3P_1\rangle \quad (\text{with } \alpha^2+\beta^2=1), \tag{1}$$

TABLE I. Singlet-triplet mixing coefficients α and β for the $(^2P_{1/2})^1S[\frac{1}{2}]_1$ and $(^2P_{3/2})^1S[\frac{3}{2}]_1$ excited states in the heavy rare gases. Resonance wavelengths for each state are also shown.

Gas	α	β	α^2	β^2	λ $(j=\frac{1}{2})$ (nm)	λ $(j=\frac{3}{2})$ (nm)
Neon	0.964	0.266	0.929	0.071	73.6	74.4
Argon	0.893	−0.450	0.797	0.203	104.8	106.7
Krypton	−0.683	0.730	0.467	0.533	116.5	123.6
Xenon	−0.645	0.764	0.416	0.584	129.6	147.0

*Present address: MS183-601, Jet Propulsion Laboratory, Pasadena, CA 91109.
†Present address: 35 Lodge Ave., Winnipeg, Manitoba, Canada R3J OR4.

TABLE II. Intensity relations for various isotopes I. It has been assumed that cross sections for $M_J=\pm1$ are identical.

I	$I_{\parallel}/C_0A(1\rightarrow0)$	$I_{\perp}/C_0A(1\rightarrow0)$
0	$Q(1,0)$	$Q(1,1)$
$\frac{1}{2}$	$\frac{1}{9}[5Q(1,0)+4Q(1,1)]$	$\frac{1}{9}[2Q(1,0)+7Q(1,1)]$
$\frac{3}{2}$	$\frac{1}{450}[224Q(1,0)+226Q(1,1)]$	$\frac{1}{450}[113Q(1,0)+337Q(1,1)]$
$\frac{9}{2}$	$\frac{1}{37125}[17521Q(1,0)+19604Q(1,1)]$	$\frac{1}{37125}[9802Q(1,0)+27323Q(1,1)]$

where α and β for the $J=1$ excited states are given for each gas in Table I]. The wavelengths of the resonance transitions are also indicated. It can be seen that the more massive rare gases (Kr and Xe) can be viewed as nearly equally mixed ^3P and ^1P states, while the lighter rare gases (Ne and Ar) can be viewed as nearly ''pure'' ^3P or ^1P. This feature along with the increasing ion core energy-level splittings as one progresses up the periodic table suggests we should see systematic changes in the polarization of the two resonance ($J=1\rightarrow J=0$) lines as we progress toward more massive targets since the position of resonances and cascading states associated with each ion core ($j=\frac{1}{2},\ \frac{3}{2}$) will shift relative to each other due to the ion core splitting.

The threshold polarization predictions outlined in II are valid for Ar but not for Kr and Xe because they contain significant amounts of naturally occurring isotopes with $I\neq0$. Using the theory of Percival and Seaton [9] and taking into account the different isotopes [10] predictions on the threshold polarization can be made.

To determine the polarization for a mixed species it is necessary to average $I_{\parallel}$ and $I_{\perp}$ (*not* the polarizations) resulting from each isotope. This results in the following relation:

$$P=\frac{\Sigma_I w(I)[I_{\parallel}(I)-I_{\perp}(I)]}{\Sigma_I w(I)[I_{\parallel}(I)+I_{\perp}(I)]}, \tag{2}$$

where $I_{\parallel,\perp}(I)$ are the intensities of the light measured in a direction perpendicular to the electron beam with electric vectors parallel and perpendicular, respectively, to the e-beam (quantization) direction for isotope I and $w(I)$ is the percentage of the total population of isotope I. Table II shows the relationship between the parallel and perpendicular intensities of the $J=1\rightarrow J=0$ transition and the excitation cross sections for the $M_J=0$ and $|M_J|=1$ levels of the $J=1$ state for different isotopes (I). C_0 is a constant and $A(1\rightarrow0)$ is the total emission probability for this transition. Substituting the relations in Table II into Eq. (2) yields

$$P=\frac{H[Q(1,0)-Q(1,1)]}{h_0Q(1,0)+h_1Q(1,1)}, \tag{3}$$

where H, h_0, and h_1 are constants (given in Table III). For singlet (triplet) excitation only $Q(1,0)$ [$Q(1,1)$] is excited at threshold (see II) and therefore $P_{\rm th}=H/h_0(-H/h_1)$.

Perturbations in the polarization due to negative-ion resonances have been calculated as outlined in II with the following modification: if nonzero nuclear spin (I) is present, as is the case for krypton and xenon, then Eqs. (13a) and (13b) of Ref. [11] must be modified (see Appendix of Ref. [12]) by replacing $(1/\gamma)\langle T(J)^{+}_{KQ}\rangle$ with $G(L)^{I}_{KQ}\langle T(J)^{+}_{KQ}\rangle$ where $G(L)^{I}_{K}$ is the same as $G(L)_K$ in Hammond *et al.* [13]. If more than one isotope is present, then $G(L)^{I}_{K}$ must be averaged over all I. For $I=0$ (e.g., Ne and Ar), $G(L)^{0}_{0}=G(L)^{0}_{2}=1/\gamma$ and the equations used in II result. Therefore the calculated polarizations for neon and argon are the same, but for krypton and xenon, averaged values of $G(L)^{I}_{2}$ must be used because of the different I for the isotopes [note that $G(L)^{I}_{0}=1/\gamma$ for all I]. The appropriate values for $\overline{G_2}$ are indicated in Tables IV and V along with the calculated polarizations. Note that these calculations assume that the negative-ion resonance is dominating the excitation. In practice this will not be the case except in rare circumstances. No theoretical calculations of polarization fractions for heavy rare-gas resonance radiation are available apart from the threshold values discussed earlier.

III. EXPERIMENT

Full discussions of the two sets of apparatus are presented in I and in Hammond *et al.* [13], and therefore only details relevant to the present measurements are outlined here. For the energy-selected measurements electron-beam currents were typically 30 nA with an energy spread of approximately 160 meV. For the unselected gun typical currents were 25 μA with a resolution of $\sim$1 eV. The measured intensities ($I^m_{\parallel}$,$I^m_{\perp}$) are related to the true values ($I_{\parallel}$,$I_{\perp}$) by Eq. (6)

TABLE III. Polarization function coefficients and threshold values for singlet ($P^s_{\rm th}$) and triplet ($P^t_{\rm th}$) excitation.

Isotope	I	%	H	h_0	h_1	$P^s_{\rm th}$	$P^t_{\rm th}$
Xe^{129}	$\frac{1}{2}$	26.4					
Xe^{131}	$\frac{3}{2}$	21.2	0.664	0.888	1.112	0.748	−0.597
Xe[a]	0	52.4					
Kr^{83}	$\frac{9}{2}$	11.5	0.909	0.970	1.030	0.937	−0.882
Kr[a]	0	88.5					

[a]All other occurring isotopes.

TABLE IV. VUV polarization fractions for the heavy rare gases resulting from the formation of the negative-ion resonance $(j=\frac{1}{2})^{2S+1}L[K]_J$, which decays to $(j=\frac{1}{2})^2S[1/2]_1$. $\overline{G_2}$ is the average over nuclear spin I of the perturbation coefficients $G(L)^I_2$ (see Ref. [11]). l_0 (l_1) is the orbital angular momentum of the incoming (outgoing) electron. For resonance nomenclature see Ref. [18].

Resonant state $(j=\frac{1}{2})$	K	J	l_0	l_1	Polarization $\overline{G_2}=1$ (Ne,Ar)	$\overline{G_2}=0.909$ (Kr)	$\overline{G_2}=0.664$ (Xe)
^3P (b and e)	$\frac{1}{2}$	$\frac{1}{2}$	0	1	0	0	0
	$\frac{3}{2}$	$\frac{1}{2}$	0	1	0	0	0
	$\frac{1}{2}$	$\frac{3}{2}$	2	1	−0.428	−0.385	−0.271
	$\frac{3}{2}$	$\frac{3}{2}$	2	1	0.558	0.516	0.395
	$\frac{3}{2}$	$\frac{5}{2}$	2	1	0.500	0.461	0.352
^1P (c)	$\frac{1}{2}$	$\frac{1}{2}$	0	1	0	0	0
	$\frac{3}{2}$	$\frac{3}{2}$	2	1	0	0	0
^1S (d_2 and f_2)	$\frac{1}{2}$	$\frac{1}{2}$	1	0	0	0	0
^1D (e)	$\frac{3}{2}$	$\frac{3}{2}$	1	2	0	0	0
	$\frac{5}{2}$	$\frac{5}{2}$	3	2	0	0	0

from I. The efficiency (η) of the single mirror polarizer used for the near-threshold measurements was obtained by normalizing these data to the higher-energy data where multiple mirror polarizers were used to make the measurements insensitive to the mirror efficiency (see Hammond *et al.* [13]).

Studies of the variation of P with gas pressure were carried out to ensure freedom from depolarizing effects such as imprisonment of resonance radiation. This meant that the background pressure in the system did not exceed 1.2×10^{-7}, 1.7×10^{-7}, and 2.1×10^{-7} torr for Ar, Kr, and Xe, respectively, for the energy-selected measurements when the gas beam was operational. Similar criteria applied for the measurements made with the unselected gun. Background effects due, for example, to small contributions to the measured signals from the background gas in the system, were accounted for as discussed by Hammond *et al.* [13]. The base pressure

TABLE V. VUV polarization fractions for the heavy rare gases resulting from the formation of the negative-ion resonance $(j=\frac{3}{2})^{2S+1}L[K]_J$, which decays to $(j=\frac{3}{2})^2S[3/2]_1$. G_2 is the average of the perturbation coefficients $G(L)^I_2$ over nuclear spin I (see Ref. [11]). l_0 (l_1) is the orbital angular momentum of the incoming (outgoing) electron. For resonance nomenclature see Ref. [18].

Resonant state $(j=\frac{3}{2})$	K	J	l_0	l_1	Polarization $\overline{G_2}=1$ (Ne,Ar)	$\overline{G_2}=0.909$ (Kr)	$\overline{G_2}=0.664$ (Xe)
^3P (b and e)	$\frac{1}{2}$	$\frac{1}{2}$	1	1	0	0	0
	$\frac{3}{2}$	$\frac{1}{2}$	1	1	0	0	0
	$\frac{1}{2}$	$\frac{3}{2}$	1	1	−0.428	−0.385	−0.271
	$\frac{3}{2}$	$\frac{3}{2}$	1	1	−0.698	−0.622	−0.430
	$\frac{5}{2}$	$\frac{3}{2}$	1	1	0.447	0.412	0.312
	$\frac{3}{2}$	$\frac{5}{2}$	3	1	0.500	0.461	0.352
	$\frac{5}{2}$	$\frac{5}{2}$	3	1	0.500	0.461	0.352
^1P (c)	$\frac{1}{2}$	$\frac{1}{2}$	0	1	0	0	0
	$\frac{3}{2}$	$\frac{3}{2}$	2	1	0.143	0.130	0.096
	$\frac{5}{2}$	$\frac{5}{2}$	2	1	0.500	0.461	0.352
^1S (d_1 and f_1)	$\frac{3}{2}$	$\frac{3}{2}$	1	0	0.600	0.555	0.427
^1D (e)	$\frac{1}{2}$	$\frac{1}{2}$	1	2	0	0	0
	$\frac{3}{2}$	$\frac{3}{2}$	1	2	−0.529	−0.473	−0.332
	$\frac{5}{2}$	$\frac{5}{2}$	3	2	−0.088	−0.080	−0.058
	$\frac{7}{2}$	$\frac{7}{2}$	3	2	0.455	0.418	0.318

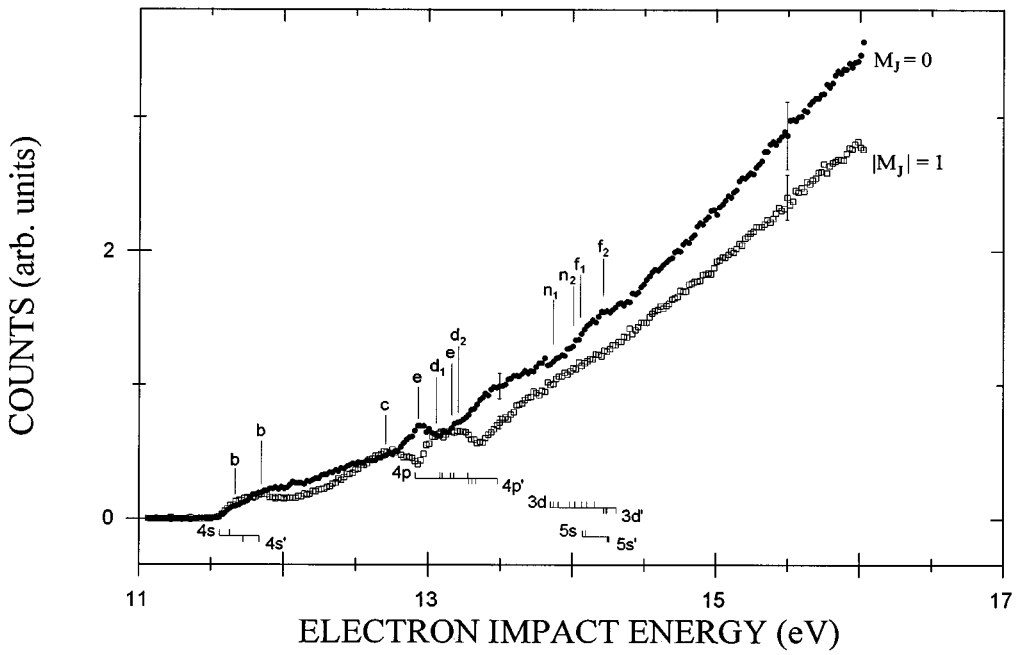

FIG. 1. Sublevel excitation functions for argon as a function of electron-impact energy. The present data were obtained with an energy-selected gun. The data have been corrected for the polarization sensitivity of the analyzer. $M_J=0$ and $|M_J|=1$ curves refer to $I_{\|}$ and $I_{\perp}$, respectively (see text). Positions of relevant negative-ion states are identified by lower-case letters [15,18] and are indicated above the curves. Positions of relevant neutral states are indicated below the curves. Typical errors are shown at 13.5 and 15.5 eV and are discussed in the text. Errors within the first 2 eV of threshold are on the order of the data point size.

without the target gas being introduced was 2×10^{-7} torr Errors were estimated as discussed in I.

IV. RESULTS AND DISCUSSION

A. Argon

The energy-selected, near-threshold, corrected VUV data are shown in Fig. 1 with the resulting polarization function presented in Fig. 2. The data points below the threshold have been set to zero for the sake of clarity. The polarization curve was calibrated to the data obtained with the unselected gun at 16 eV, since this is a linear region in the polarization function and a value of 0.478 was determined for η. The unselected data and those of Dassen *et al.* [3] are also presented for comparison. Note that Dassen *et al.* used an LiF filter to suppress the $(^1P_1-{}^1S_0)$ 104.8 nm line and therefore their data reflect the polarization of the $(^3P_1-{}^1S_0)$ 106.7-nm line only. We have performed unselected measurements with and without an LiF filter (see below).

From the VUV data (Fig. 1), the effects of the negative-ion resonances on each channel are very clear. In the $|M_J|=1$ channel ($I_{\perp}$) the *b*, *c*, and *d* resonances are prominent, while in the $M_J=0$ channel ($I_{\|}$) the *e* resonance observed at 12.93 eV by Brunt *et al.* [14] is evident, as is a broad feature at 14.15 eV. Note that although the *c* resonance is clearly observed in the $|M_J|=1$ channel, it is barely detectable in total emission spectra ($I_{\|}+I_{\perp}$). This explains why Brunt *et al.* [14], who measured the total UV flux from Ar saw little sign of the resonance even though they had more than adequate energy resolution.

The polarization function reflects the predominance of the resonances in one channel or the other. Near threshold, the presence of the *b* resonances makes it difficult to determine the trend of the polarization with the present energy resolution. Since the ^3P character is dominant (see Table I) the exchange mechanism is expected to dominate as it did in neon, and therefore the polarization should tend toward -1. However, the polarization is clearly perturbed by the *b* resonances. For example, a *b* resonance is observed [15] in the metastable channel at 11.631 meV, just 8 meV above the threshold of the first VUV emitting state with another *b* resonance 44 meV higher in energy. Ohja *et al.* [16] have calculated excitation cross sections for argon assuming an *LS* configuration, and their results show that the *b* resonances perturb the excitation of the $4p^5 4s\ {}^3P^o$ state.

Before the onset of the second VUV-emitting state the polarization begins to rise sharply toward a maximum value of 0.30. Since the cross section of the $^2P_{3/2}4s[3/2]_1$ state should be significantly larger than $^2P_{1/2}4s[1/2]_1$ in this region, the effect of the $^2P_{1/2}4s[1/2]_1$ state on the polarization should be minimal unless it is strongly polarized near threshold. In support of this are the unselected measurements made of the VUV polarization with and without an LiF filter. Each data set shows a different trend at threshold. The LiF filter suppresses the 104.8-nm line and therefore only the 106.7-nm line is observed. The LiF data show the polarization dropping to 0, which is consistent with the higher-resolution data since, at threshold, it also contains only the 106.7-nm line. The polarization data collected without the LiF filter are consistently higher. This could be attributed to observation of the decay of the $^2P_{1/2}4s[1/2]_1$ state, which is predominantly ^1P in character and therefore has a $+1$ threshold polarization value (see earlier threshold angular-momentum arguments). This would suggest that the excita-

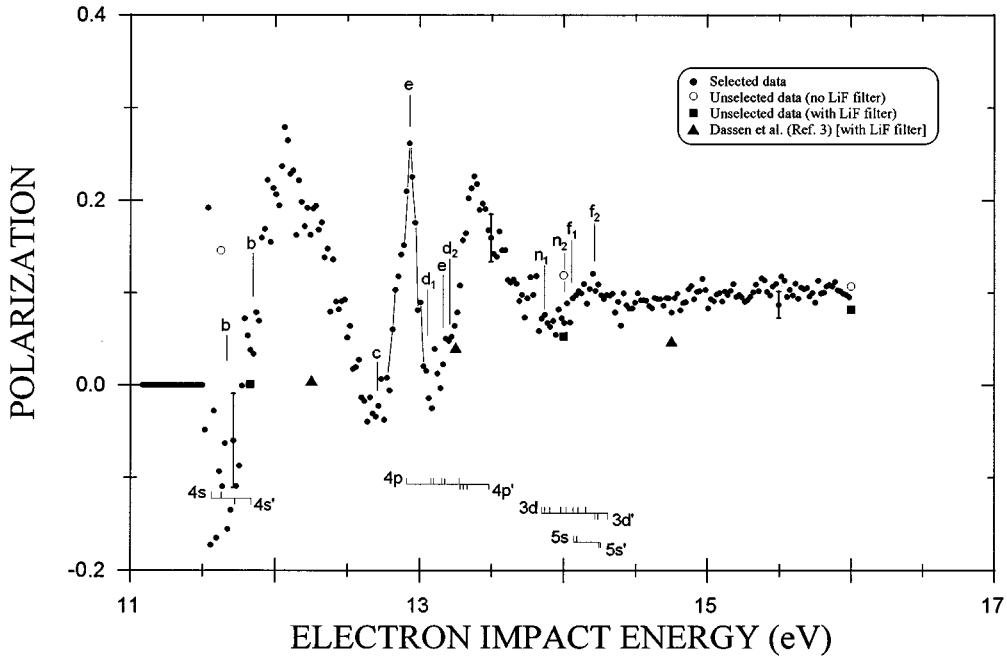

FIG. 2. Polarization function for the VUV radiation from argon as a function of electron-impact energy. The present data were obtained with an energy-selected gun. Data from the lower-resolution work of Dassen *et al.* [3] are indicated on the graph along with the present results (see text). Positions of relevant negative-ion states are identified by lower-case letters [15,18] and are indicated above the curves. Positions of relevant neutral states are indicated below the curves. Typical error limits are shown at threshold, 13.5, and 15.5 eV and are discussed in the text.

tion of the $^2P_{1/2}4s[1/2]_1$ state is significant near threshold. The measurements of Ajello *et al.* [17] indicate that at 12 eV, excitation of the $^2P_{1/2}4s[1/2]_1$ state is responsible for 26% of the total VUV emission. Dassen *et al.*'s [3] measurements using an LiF filter are in agreement with the present data.

In the region between 12.0 and 12.5 eV, where the polarization should be unaffected by resonance excitation, the polarization stays significantly positive. This is in contrast to the situation in neon where negative polarization values were observed at energies above the threshold resonance region. The difference may be due to the fact that in Ar a larger deviation from a pure LS coupling scheme occurs. One might conclude that exchange excitation is not as significant in argon or perhaps that the exchange mechanism drops off more rapidly with increasing energy above threshold than in the case of neon.

After the maximum observed at 12.2 eV, the polarization then experiences the effects of the c resonance and drops to 0. The width of the c resonance has not been determined experimentally but it is seen to be very broad in metastable data [15] as well as in our $|M_J|=1$ data. This drop to 0 is supported by the present calculations shown in Tables IV and V. Note that the designation of the c resonance is not agreed upon. The grandparent model predicts that these should be ^1P resonances, but theoretical calculations [16] indicate that this resonance could have a ^1D configuration. Buckman and Clark [18] suggest that this state may in fact be a mixture of both. The present data suggest that a strong ^1D admixture, based on an incoming p wave and an outgoing d wave, is likely due to the fact that this resonance would strongly enhance the $|M_J|=1$ cross section, as is observed (see Table V).

The analysis of the polarization function becomes more difficult at energies above the c resonance because of the overlap of numerous resonances. Note that the overlap of the c resonance with the e and d resonances is not due to lack of experimental resolution but results from the natural widths of these resonances. After the center of the c resonance, the e resonance appears and causes the polarization function to rise sharply. A maximum value of 0.25 is reached, followed by a drop to 0 that can be explained by the presence of the d resonances that are located here. After the d_2 resonance, the polarization rises to a maximum value of 0.20 and then falls to a value of 0.05. This shape in the polarization curve was also observed in neon where the d resonances appeared as a dip in the midst of a broader ''bump'' and therefore this broad ''bump'' may be due to e resonances of ^2P character. Alternatively, the positive excursion of the polarization at energies higher than the d resonances may reflect the fact that the so-called ''singlet'' transition is beginning to dominate the excitation process. In support of this is the fact that the polarization data taken with the LiF filter (triplet line only) lie lower on average than the integrated data (see Fig. 2). The influence of cascade from the $4p$ levels in this region should not be overlooked either.

The polarization function shows a slight bump centered at 14.15 eV that lies within the range of the n_1, n_2, f_1, and f_2 resonances as well as the $3d$ and $5s$ excited states. Table V indicates that the f_1 resonance should lead to positive polarization values, as are observed. The small perturbation to the polarization may reflect the fact that the resonance structure

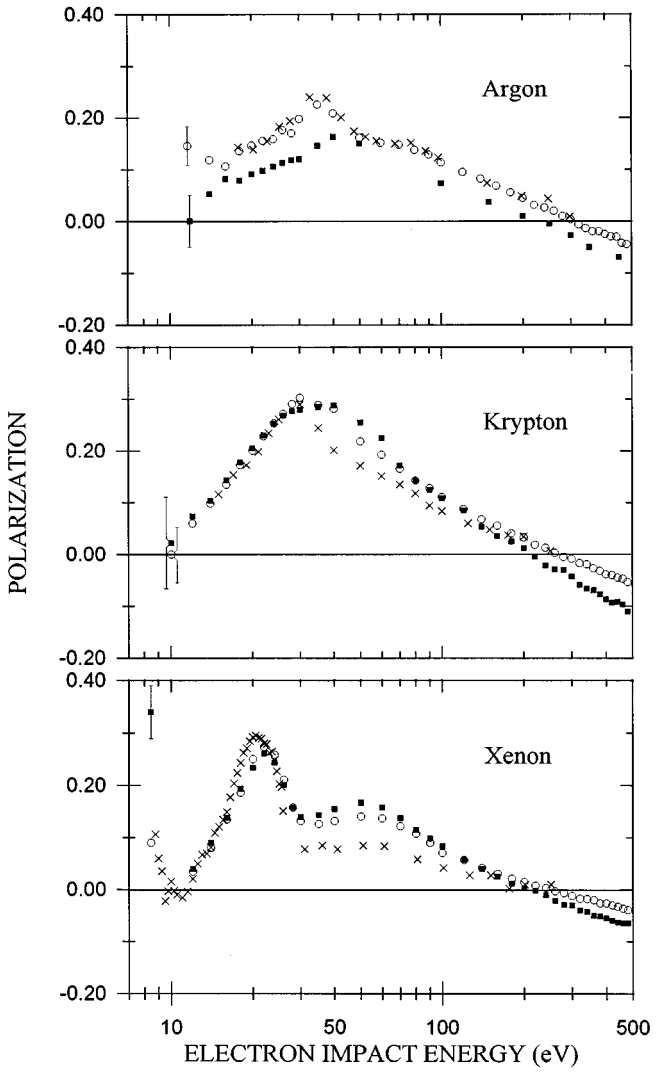

FIG. 3. Integrated VUV polarization functions for argon, krypton, and xenon as a function of electron-impact energy. The present data were obtained with an unselected electron gun. Circles, present data (no LiF filter); squares, present data (LiF filter used); ×, Uhrig *et al.* [6,7]. The errors in the present data (see Table VI) were on the order of the data point size except at threshold where error limits are shown.

is relatively small compared to the background. From 14.4 to 16 eV the polarization has a slight linear increase. It is interesting to note that by 15 eV, it is estimated from data presented by Ajello *et al.* [17] that the cascade to both $3p^5\,4s,4s'$ $(J=1)$ VUV emitting states represents more than half of the signal. While Ballou and Lin [19] did not observe the cascading emissions to be significantly polarized, it is difficult to estimate the effect of cascade because no detailed measurements of the polarization of these features have been reported.

The polarization of argon above the threshold region, obtained with the unselected gun, is shown in Fig. 3 and tabulated in Table VI for selected energies from threshold to 480 eV. These data are taken from a smooth curve fitted through the experimental points. This is more difficult to analyze than neon [13] because of the abundance of spectral features which contribute to the observed signal (Ajello *et al.* [17] and McConkey and Donaldson [20]). Above the threshold region, the polarization decreases to a minimum at ~16 eV, rises to a peak at ~35 eV, and then drops to a ''shoulder'' feature at ~60 eV. It then steadily decreases and crosses zero at 307±10 eV.

The low polarization below 30 eV may be due, in part, to a large cascade contribution to the argon resonance lines as well as the presence of the 106.7-nm line, resulting from the $^2P_{3/2}4s[3/2]_1$ state and other lines. The many spectral components have been examined by McConkey and Donaldson [20] at 100 eV and Ajello *et al.* [17] at 200 eV with both spectra indicating strong Ar I and Ar II constituents. Note that below 29.2 eV only Ar I lines are observed. No energy-selected measurements could be carried out using the LiF window because the chamber was heated to improve electron gun performance. This shifted the temperature-dependant cutoff frequency of the LiF filter so that both resonance lines were suppressed. Excellent agreement with the data of Uhrig *et al.* [6] is observed over the whole energy range.

The polarization curve measured with an LiF filter is lower in value than the unfiltered data, indicating that the radiation lying below 105 nm at low energy (predominantly 104.8 nm) is more positively polarized. The filtered data cross the zero polarization axis at 218±15 eV, which is 89 eV lower than for the unfiltered data.

B. Krypton

In krypton the main sources of resonance radiation are the 116.5-nm and the 123.6-nm lines, which result from the decay of the $^2P_{1/2}5s[1/2]_1$ and $^2P_{3/2}5s[3/2]_1$ states, respectively. The energy-selected, near-threshold, corrected VUV data are shown in Fig. 4 with the resulting polarization function presented in Fig. 5. The data points below the threshold have been set to zero for the sake of clarity. The polarization curve was calibrated to data obtained with the unselected gun at 14 eV since this is a linear region in the polarization function. A value of 0.649 was determined for η of the single mirror analyzer in this spectral region.

Krypton has a large spin-orbit splitting (666 meV) that results in the negative-ion resonance pairs being well separated. Also, jj coupling becomes more appropriate in describing the excited states of the noble gases as the mass increases. Thus krypton presents an opportunity to evaluate the effectiveness of the coupling schemes used to describe the various excited states. Another feature of krypton is the nearly equal contributions of ^3P and ^1P to both $4p^5 5s(J=1)$ VUV-emitting levels and, therefore, the overall configuration cannot be approximated by singlet or triplet states as in neon and argon. Finally, the nuclear spin of the isotopes are not all zero as with helium, neon, and argon (see Table III), so the measured polarization will be reduced as discussed earlier. For example, the threshold polarization for direct excitation becomes 0.937, while for pure exchange excitation the threshold polarization would be -0.882.

The VUV spectrum shows the presence of the a_2 resonance $(4p^5 5s^2)$, which lies 86 meV above the $^2P_{3/2}5s[3/2]_1$ threshold. In argon and neon the corresponding structures occurred lower in energy than the $3p^5 4s$ and $2p^5 3s$ states, respectively, and therefore were not observed. The a_2 resonance dominates the spectrum near threshold. This is quite

TABLE VI. Polarizations and errors for integrated VUV radiation from argon, krypton, and xenon. The measurements were made with the unselected electron gun (see text).

Energy (eV)	Argon		Krypton		Xenon	
	Polarization	Error	Polarization	Error	Polarization	Error
Threshold	0.146	0.037	0.000	0.050	0.090	0.030
12			0.060	0.007	0.035	0.004
14	0.119	0.010	0.099	0.004	0.081	0.003
16	0.107	0.005	0.135	0.003	0.135	0.003
18	0.136	0.004	0.173	0.003	0.187	0.004
20	0.147	0.004	0.201	0.004	0.250	0.004
22	0.146	0.004	0.229	0.004	0.274	0.005
24	0.159	0.004	0.254	0.004	0.259	0.004
26	0.177	0.005	0.272	0.005	0.211	0.004
28	0.170	0.004	0.291	0.005	0.158	0.003
30	0.198	0.004	0.303	0.005	0.132	0.003
35	0.226	0.004	0.289	0.005	0.127	0.003
40	0.209	0.004	0.282	0.005	0.132	0.003
50	0.162	0.004	0.219	0.004	0.141	0.003
60	0.152	0.004	0.193	0.004	0.137	0.003
70	0.148	0.004	0.166	0.003	0.122	0.003
80	0.138	0.004	0.143	0.003	0.108	0.003
90	0.129	0.004	0.128	0.003	0.090	0.003
100	0.114	0.004	0.111	0.003	0.071	0.003
120	0.095	0.004	0.088	0.003	0.057	0.003
140	0.082	0.004	0.068	0.003	0.042	0.003
160	0.069	0.004	0.056	0.003	0.031	0.003
180	0.056	0.004	0.041	0.003	0.022	0.003
200	0.045	0.004	0.033	0.003	0.015	0.003
220	0.032	0.004	0.019	0.003	0.008	0.003
240	0.027	0.004	0.013	0.003	0.004	0.003
260	0.020	0.004	0.003	0.003	−0.003	0.003
280	0.010	0.004	−0.005	0.003	−0.006	0.003
300	0.004	0.003	−0.008	0.003	−0.012	0.003
320	−0.006	0.003	−0.017	0.003	−0.017	0.003
340	−0.013	0.004	−0.019	0.003	−0.018	0.003
360	−0.019	0.004	−0.027	0.003	−0.020	0.003
380	−0.019	0.004	−0.032	0.003	−0.026	0.003
400	−0.025	0.004	−0.038	0.003	−0.026	0.003
420	−0.029	0.004	−0.040	0.003	−0.030	0.003
440	−0.030	0.004	−0.045	0.003	−0.033	0.003
460	−0.042	0.004	−0.047	0.003	−0.036	0.003
480	−0.044	0.004	−0.053	0.003	−0.039	0.003

surprising since the decay of this resonance to the $^2P_{3/2}5s[3/2]_1$ state requires a change in the ion core angular momentum. Decay of the a_2 resonance to the metastable state is also observed [15], but it has a significantly reduced signal. Note that in the present data the center of the resonance is not the same in both channels but differs by 20 meV, the parallel channel being lower. This may be a result of the presence of an unresolved b resonance, which was observed in the metastable spectrum [15] at 10.039 eV (6 meV above the $^2P_{3/2}5s[3/2]_1$ threshold) and has a full width at half maximum (FWHM) of 130 meV.

At energies higher than the a_2 resonance, the spectrum does not have the prominent features observed in neon and argon. This is due to the fact that the resonances are small and narrow (see data of Brunt *et al.* [14]) and the resolution of the electron beam of the present experiment is relatively large. The corrected $M_J=0$ data do show the presence of the broad c resonance at 11.6 eV and the d_1 and d_2 resonances appear as dips, as was the case in argon.

The polarization function (Fig. 5) clearly indicates the presence of well-defined resonant structure. At threshold it can be seen that the polarization curve is tending toward negative values, indicating that exchange is important in this energy region. The polarization quickly rises to a value of 0.08 and then falls to −0.38. Note that the position of the a_2 resonance does not coincide with the center of the dip in the polarization. This reflects the nonalignment of the centers of the peaks observed in the parallel and perpendicular channels

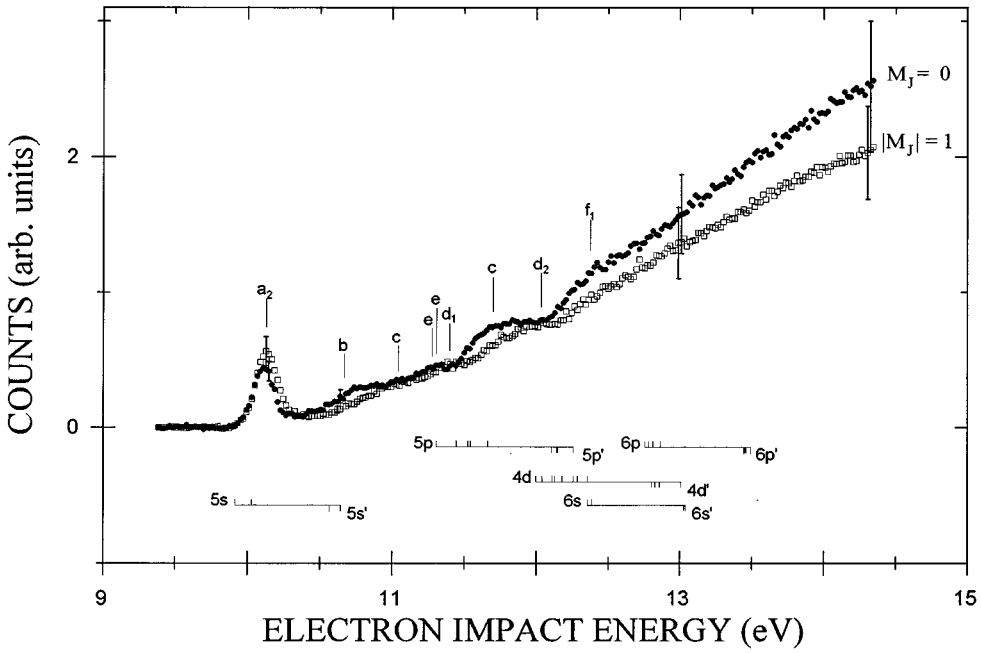

FIG. 4. Sublevel excitation functions for krypton as a function of electron-impact energy. The present data were obtained with an energy-selected gun. The data have been corrected for the polarization sensitivity of the analyzer. $M_J=0$ and $|M_J|=1$ curves refer to $I_{\parallel}$ and $I_{\perp}$, respectively (see text). Positions of relevant negative-ion states are identified by lower-case letters [15,18] and are indicated above the curves. Positions of relevant neutral states are indicated below the curves. Typical errors are shown at 10.2, 13, and 14.3 eV and are discussed in the text.

(Fig. 4). The quick rise to 0.08 near threshold is consistent with polarizations measured for the *b* resonance in neon. It appears as if the two resonances are competing for dominance in this region very close to threshold.

After reaching a minimum at 10.2 eV, the polarization function rises to a maximum value of 0.25 at 10.6 eV where the *b* resonance and the $^2P_{1/2}5s[1/2]_1$ state are located. Since the direct excitation of the $^2P_{1/2}5s[1/2]_1$ state is not expected to contribute significantly near threshold, the rise in polarization is likely due to the *b* resonance. After the *b* resonance, the polarization falls to $\sim$0 at 11 eV, which is in the vicinity of the *c* resonance (11.12 eV). The polarization remains constant until the location of the d_1 resonance, where it drops below 0. The effect of the *e* resonances at 11.29 and 11.32 eV is not clear due to the statistical scatter in the data. The polarization rises to a value of 0.10 after the d_1 resonance and then declines to 0 under the successive influences of the *c* (11.77 eV) and d_2 resonances. After the d_2 resonance, the polarization curve exhibits a broad bump at the location of the 6*s* levels and the f_1 resonance. This is very similar to the behavior found with argon.

Our measurements made with the unselected gun (see Table VI and Fig. 3) and those of Uhrig *et al.* [6] agree with the present data. The same cannot be said for the data of Al-Shamma and Kleinpoppen [4], which are significantly lower in value. However, these authors now believe their data to be in error [21].

The polarization above the near-threshold region (Fig. 3) rises to a peak at $\sim$30 eV and then decreases steadily to zero at 272$\pm$10 eV. Figure 3 also shows the polarization measured using a LiF filter that has a maximum at $\sim$32 eV and a zero crossover at 212$\pm$10 eV. The polarization functions coincide with each other over the range from threshold to 26.8 eV. This would indicate that spectral features, which would be suppressed by the LiF filter, are not significant in this energy region (i.e., the polarization function is dominated by $4p$-$5s$ transitions). Above 26.8 eV, Kr II lines begin to influence the polarization of the unfiltered data, since their wavelength is less than 100 nm and thus the polarization functions begin to diverge. We note that in this energy range our data also diverge from those of Uhrig *et al.* [6]. Most likely this is due to different relative detection sensitivities for the Kr II lines at 91.7 and 96.5 nm.

C. Xenon

The energy-selected, near-threshold VUV spectrum of xenon was measured with and without a BaF_2 filter. The BaF_2 filter has a temperature-dependent cutoff that lies between the 129.6-nm line ($(^2P_{1/2})6s[1/2]_1$) and the 147.0-nm line ($(^2P_{3/2})6s[3/2]_1$). The transmission of the 147.0-nm line fortunately increases with temperature (allowing the chamber to be heated for maximum current production and beam stability) and is roughly 20% [22]. Since very few differences were observed between the data sets obtained with and without the filter, only the filtered data will be presented here.

The energy-selected, near-threshold, corrected VUV data are shown in Fig. 6, with the resulting polarization function presented in Fig. 7. The data points below the threshold have been set to zero for the sake of clarity. The data were normalized to measurements made with the unselected gun in a fashion similar to that used for Ar and Kr. Based on this normalization, η for the single mirror analyzer was found to be 0.664 in this spectral region. Identical polarization functions were obtained in the low-energy region with and without the BaF_2 filter. This reflects the dominance of the

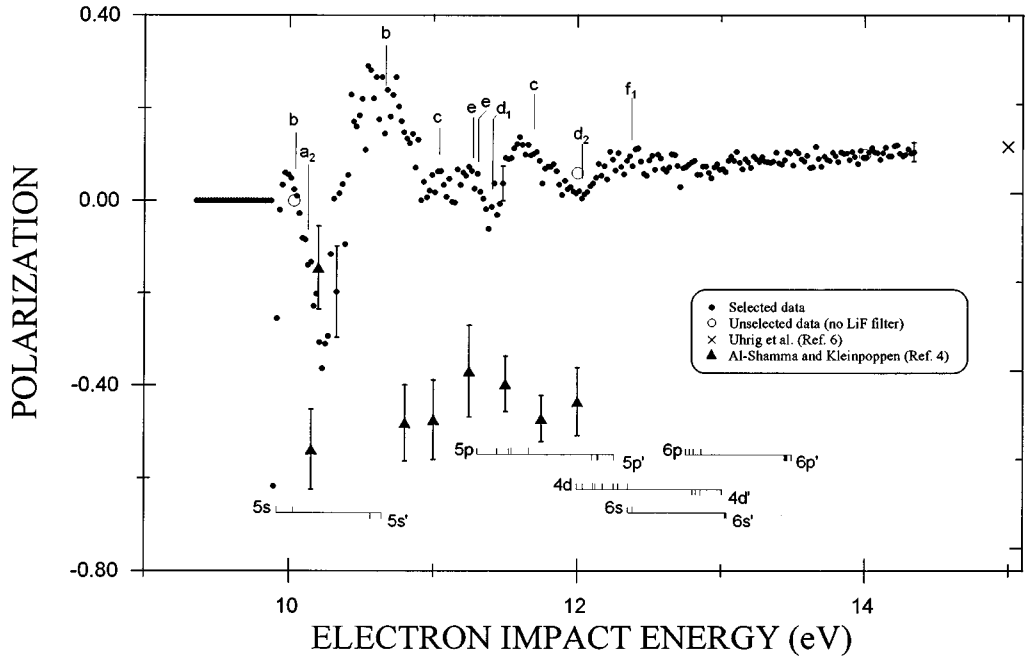

FIG. 5. Polarization function for the VUV radiation from krypton as a function of electron-impact energy. The present data were obtained with an energy-selected gun. Data from the lower-resolution work of Uhrig *et al.* [6] and Al-shamma and Kleinpoppen [4] are indicated on the graph along with the present results (see text). Positions of relevant negative-ion states are identified by lower-case letters [15,18] and are indicated above the curves. Positions of relevant neutral states are indicated below the curves. Typical error limits are shown at 10.4, 11.5, and 14.5 eV and are discussed in the text.

$^2P_{3/2}6s[3/2]_1$ state in this energy region.

The spin-orbit splitting (1307 meV) of the ion core is the largest of the rare gases studied in the present work and therefore the resonance structures based on the two different cores will be well separated. Like krypton, the VUV-emitting states cannot be classified as ^3P or ^1P (see Table I) but are roughly a 60-40 mixture of the two. The a_2 resonance ($5p^5 6s^2$), observed near threshold in krypton, now lies approximately 740 meV above the first VUV emitting state [18], which results in it being a much broader and weaker resonance. Hence it is difficult to distinguish due to the presence of the c resonance at 9.18 eV. Finally, only VUV emissions from the $^2P_{3/2}6s[3/2]_1$ state are being monitored because of the BaF_2 window placed in front of the photon detector.

The VUV spectrum (Fig. 6) clearly shows the effect that the resonances have on populating the magnetic sublevels of the $^2P_{3/2}6s[3/2]_1$ state. In the threshold region, a pronounced shoulder appears in the perpendicular channel near the location of the b resonance at 8.43 eV. In the metastable measurements of Buckman *et al.* [15] a b resonance was observed 100 meV below the threshold for the $^2P_{3/2}6s[3/2]_1$, which could have a minor influence on the relative populations at threshold if its width exceeds 100 meV. Observations of the other heavy rare gases indicate that this is possible.

The effect of the c resonance in populating the $|M_J|=1$ channel is visible at 9.08 eV. Above the c resonance there are several resonances clustered together, including another c resonance at 9.36 eV. Due to the energy resolution and statistical scatter the effects of each resonance are not clear. However, a dip appears in the $M_J=0$ channel where the d_1 resonance is located. Note that the onsets for the $^2P_{1/2}6s[1/2]_1$ (B_4) as well as the $6p$ neutral states are in this region as well. The opening of these channels could also be responsible for the small drop in signal observed. The effects of the n_1 resonance are seen at 9.9 eV as well as the broad feature of a third c resonance at 10.48 eV. Again statistical scatter prevents the definite identification of resonances after the c resonance (10.48 eV) but there is a hint of structure in the $M_J=0$ channel at the location of the d_2 and n_2 resonances.

The polarization function shows many of the features discussed above. As in the case of krypton the theoretical threshold polarization value for direct (exchange) excitation is less than $+1$ (-1) due to the nonzero nuclear spin (I) of its naturally occurring isotopes (see Table III). The predicted threshold polarizations are 0.748 and -0.597 for direct and exchange excitation, respectively. At threshold the polarization appears to be heading toward the pure exchange threshold value.

Above the threshold region, the polarization rises to a maximum of 0.25 and then drops to zero. The effect of the c resonance (9.18 eV) is seen to lower the polarization function to a value of -0.10. It then rises to zero possibly under the influence of the c resonance at 9.36 eV. Above the c resonance (9.36 eV) the polarization again drops below zero under the influence of the e and d_1 resonances. A broad feature in the polarization curve is observed in the region of the $6p$ and $5d$ neutral states, indicating that cascade may be significantly polarized. Also located in this region is the n_1 resonance. No other features are distinguishable in the polarization function above the n_1 resonance due to the statistical scatter in the data.

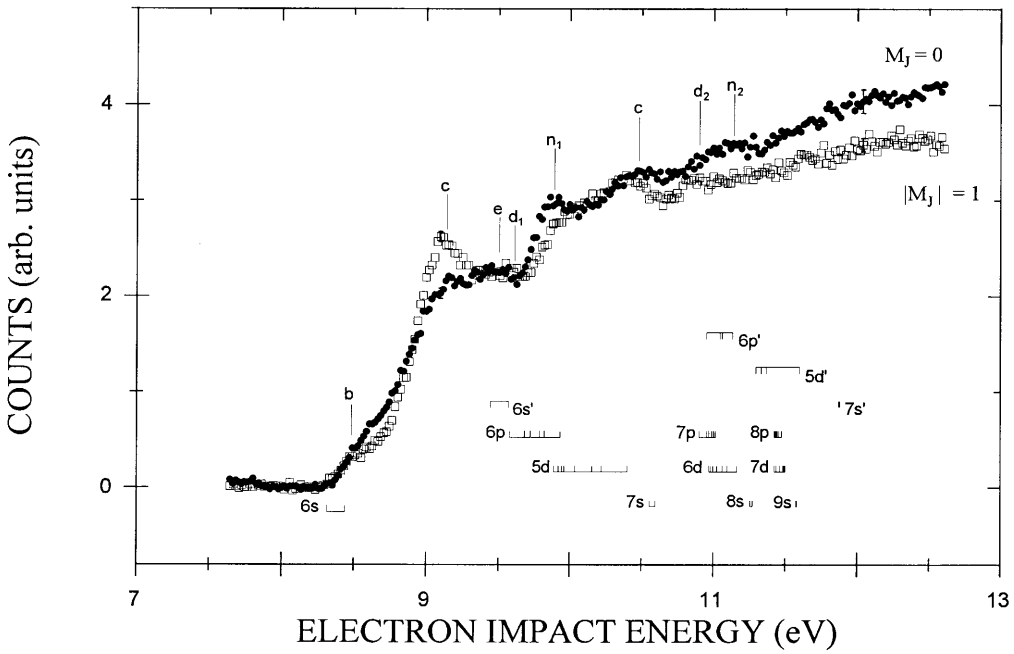

FIG. 6. Sublevel excitation functions for xenon as a function of electron-impact energy. The present data were obtained with an energy-selected gun. A BaF_2 filter has been used to suppress the 129.6-nm line. The data have been corrected for the polarization sensitivity of the analyzer. $M_J=0$ and $|M_J|=1$ curves refer to $I_\parallel$ and $I_\perp$, respectively (see text). Positions of relevant negative-ion states are identified by lower-case letters [15,18] and are indicated above the curves. Positions of relevant neutral states are indicated below the curves. The errors in the data are on the order of the data point size.

Other polarization measurements are shown in Fig. 7 and, as in the case of krypton, the data of Al-Shamma and Kleinpoppen [5] significantly differ from the present results. These authors now believe their data to be suspect [21]. Our unselected data and those of Uhrig *et al.* [7] are seen to be in very good agreement with the near-threshold data. The data of Uhrig *et al.* [7] do not show the dip centered on the *c* resonance at 9.18 eV, but this is probably a result of their poorer energy resolution (300 meV).

The polarization function resulting from the unselected data (Table VI) is shown in Fig. 3 along with the data of Uhrig *et al.* [6,7]. As the energy is increased, the polarization function rises to a maximum at ~23 eV and then drops to a minimum at ~30 eV probably due to the influence of the Xe II lines, which have an onset at 23.4 eV. The polarization curve then rises to a further maximum at ~50 eV and then decreases to cross the axis at 210±10 eV. We note that in this energy range our data also diverge from those of Uhrig *et al.* [6]. Most likely this is due to different relative detection sensitivities for the Xe II lines.

V. NEGATIVE-ION SYSTEMATICS

As suggested in the Introduction there are some similarities in the data between the heavy rare gases, most noticeably in the threshold region. The near-threshold polarization for all the gases shows a trend toward negative values indicating that exchange excitation is very important in this energy region. This finding is in agreement with measurements by Hanne *et al.* [23] for Hg, where they also observed exchange excitation dominating at threshold.

Above threshold the *b* resonances cause the polarization to rise to large positive values. Note that these resonances have total angular momentum $(J)=\frac{3}{2}, \frac{5}{2}$ and are created by incident electrons with partial waves $(l_0)\geqslant 1$. The fact that *s*-wave scattering is not responsible for the near-threshold resonances has also been observed by Wolcke *et al.* [12] in their analysis of polarized and unpolarized electrons impacting ground-state mercury. Their results show that electrons with $l_0=2$ are responsible for the formation of a negative-ion resonance with $J=\frac{5}{2}$.

The effect of the *c* resonance is not totally consistent throughout the elements, which may reflect the changing nature of this resonance as mass increases. Recall that there is some discussion on the designation of this state in argon since theoretical calculations suggest its configuration differs from that in neon [16]. In neon (II), Ar, and Xe the *c* resonances enhanced the $|M_J|=1$ channel.

The d_1 resonances $(j=\frac{3}{2})$ appear as dips in all the polarization functions. These decreases in the polarization are not consistent with the resonance polarization calculations shown in Table V $(j=\frac{3}{2})$ since the polarization is predicted to be large and positive and thus would not act to depolarize the observed radiation. Therefore it seems clear that either the grandparent model does not adequately describe the resonance or, more likely, the resonance polarization calculation needs to consider interference between the various states and alternate decay channels (i.e., changes in ion core configuration). The d_2 resonances are also observed to have a depolarizing effect.

The large number of *e* resonances are much more difficult to quantify. However, it appears that those which lie between the *c* and the *d* resonances cause the polarization to increase. This feature is clearly seen in argon and neon (II).

We note that Furst *et al.* [8], in their measurements of the

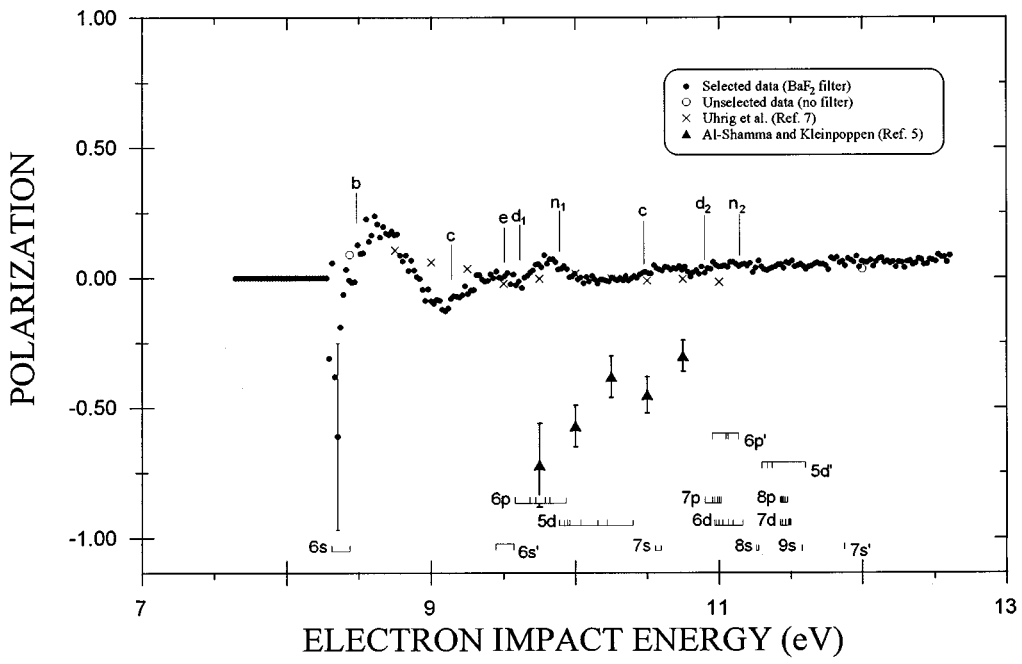

FIG. 7. Polarization function for the VUV radiation from xenon as a function of electron-impact energy. The present data were obtained with an energy-selected gun. Data from the lower-resolution work of Uhrig *et al.* [7] and Al-shamma and Kleinpoppen [5] are indicated on the graph along with the present results (see text). Positions of relevant negative ion states are identified by lower-case letters [15,18] and are indicated above the curves. Positions of relevant neutral states are indicated below the curves. A typical error limit for the threshold region is shown. The errors in the data above the threshold region are on the order of the data point size and are discussed in the text.

polarization of various visible and near-infrared transitions in the heavy rare gases, saw no indication of resonance structure. They observed threshold polarizations consistent with those predicted assuming *LS* coupling.

VI. CONCLUSIONS

The polarization function for the integrated VUV radiation resulting from electron impact on Ar, Kr, and Xe atoms has been measured from threshold to 480 eV. The lower-energy regions of the polarization functions were measured with higher-energy resolution and were observed to go toward negative values near threshold, indicating that exchange excitation is significant at these energies. Above threshold the perturbing effects of the various negative-ion resonances on the polarization functions can be seen, and predictions of the effects of these resonances on the observed polarizations have been made using a generalized Baranger-Gerjuoy theory. Above the near-threshold region, the broad features of the polarization functions have been measured and were demonstrated to depend on the spectral sensitivity of the detector. The measurements will be useful for calibration of spectral equipment.

ACKNOWLEDGMENTS

The authors are pleased to acknowledge financial assistance from the Natural Sciences and Engineering Research Council of Canada and expert technical help from the staff of the mechanical and electronic shops at Windsor. P. Hammond acknowledges the financial support of the U.K. Engineering and Physical Sciences Research Council. The authors would like to thank K. Bartschat for his helpful discussions.

[1] C. Norén, J. W. McConkey, P. Hammond, and K. Bartschat, Phys. Rev. A **53**, 1559 (1996).
[2] C. Norén and J. W. McConkey, Phys. Rev. A **53**, 3253 (1996).
[3] H. Dassen, I. C. Malcolm, and J. W. McConkey, J. Phys. B **10**, L493 (1977).
[4] S. H. Al-Shamma and H. Kleinpoppen, in *Abstracts of the Tenth International Conference on the Physics of Electronic and Atomic Collisions* (Commissariat à l'Energie Atomique, Paris, 1977), Vol. 1, p. 518.
[5] S. H. Al-Shamma and H. Kleinpoppen, J. Phys. B **11**, L367 (1978).
[6] M. Uhrig, S. Hörnemann, M. Klose, K. Becker, and G. F. Hanne, Meas. Sci. Technol. **5**, 1239 (1994).
[7] M. Uhrig, G. F. Hanne, and J. Kessler, J. Phys. B **27**, 4009 (1994).
[8] J. E. Furst, M. K. P. Wijayaratna, D. H. Madison, and T. J. Gay, Phys. Rev. A **47**, 3775 (1993).
[9] I. C. Percival and M. J. Seaton, Philos. Trans. R. Soc. London, Ser. A **251**, 113 (1958).
[10] R. A. Bonham, J. Phys. B **15**, L361 (1982).
[11] K. Bartschat, K. Blum, G. F. Hanne, and J. Kessler, J. Phys. B. **14**, 3761 (1981).

[12] A. Wolcke, K. Bartschat, K. Blum, H. Borgmann, G. F. Hanne, and J. Kessler, J. Phys. B **16**, 639 (1983).
[13] P. Hammond, W. Karras, A. G. McConkey, and J. W. McConkey, Phys. Rev. A **40**, 1804 (1989).
[14] J. N. H. Brunt, G. C. King, and F. H. Read, J. Phys. B **10**, 3781 (1977).
[15] S. J. Buckman, P. Hammond, G. C. King, and F. H. Read, J. Phys, B **16**, 4219 (1983).
[16] P. C. Ohja, P. G. Burke, and K. T. Taylor, J. Phys. B **15**, L507 (1982).
[17] J. M. Ajello, G. K. James, B. Franklin, and S. Howell, J. Phys. B **23**, 4355 (1990).
[18] S. J. Buckman and C. W. Clark, Rev. Mod. Phys. **66**, 539 (1994).
[19] J. K. Ballou and C. C. Lin, Phys. Rev. A **8**, 1797 (1973).
[20] J. W. McConkey and F. G. Donaldson, Can J. Phys. **14**, 3777 (1981).
[21] H. Kleinpoppen (private communication).
[22] J. A. R. Samson, *Techniques of Vacuum Ultraviolet Spectroscopy* (Pied, Lincoln, 1967), p. 182.
[23] G. F. Hanne, K. Wemhoff, A. Wolcke, and J. Kessler, J. Phys. B **14**, L507 (1981).